PHILOSOPHICAL TRANSACTIONS OF THE ROYAL SOCIETY A MATHEMATICAL, PHYSICAL & ENGINEERING SCIENCES

Irreversibility in quantum maps with decoherence

Ignacio García-Mata, Bernardo Casabone and Diego A. Wisniacki

Phil. Trans. R. Soc. A 2011 **369**, 278-290
doi: 10.1098/rsta.2010.0254

PHILOSOPHICAL TRANSACTIONS OF THE ROYAL SOCIETY A

Phil. Trans. R. Soc. A (2011) **369**, 278–290
doi:10.1098/rsta.2010.0254

Irreversibility in quantum maps with decoherence

By Ignacio García-Mata[1,*], Bernardo Casabone[2] and Diego A. Wisniacki[2]

[1]*Departamento de Física, Laboratorio TANDAR, Comisión Nacional de Energía Atómica, Av. del Libertador 8250, C1429BNP Buenos Aires, Argentina*
[2]*Departamento de Física, FCEyN, UBA, Pabellón 1 Ciudad Universitaria, C1428EGA Buenos Aires, Argentina*

The Boltzmann echo (BE) is a measure of irreversibility and sensitivity to perturbations for non-isolated systems. Recently, different regimes of this quantity were described for chaotic systems. There is a perturbative regime where the BE decays with a rate given by the sum of a term depending on the accuracy with which the system is time reversed and a term depending on the coupling between the system and the environment. In addition, a parameter-independent regime, characterized by the classical Lyapunov exponent, is expected. In this paper, we study the behaviour of the BE in hyperbolic maps that are in contact with different environments. We analyse the emergence of the different regimes and show that the behaviour of the decay rate of the BE is strongly dependent on the type of environment.

Keywords: quantum echoes; quantum maps; decoherence

1. Introduction

In quantum mechanics, there is no 'exponential separation' of initial conditions owing to chaotic motion because evolution is—in principle—unitary. Peres [1] proposed, as an alternative, to study the stability of quantum motion owing to perturbations in the Hamiltonian. As a consequence, the Loschmidt echo (LE) ([1–3]; see also two reviews [4,5])

$$M(t) = |\langle\psi_0|\mathrm{e}^{\mathrm{i}H_\Sigma t/\hbar}\mathrm{e}^{-\mathrm{i}Ht/\hbar}|\psi_0\rangle|^2 \tag{1.1}$$

was introduced with the purpose of characterizing the sensitivity and irreversibility arising from the chaotic nature of quantum systems. The parameter Σ denotes perturbation strength. Equation (1.1) has a dual interpretation. On the one hand, it can be interpreted as how close a state remains to itself evolving under slightly different Hamiltonians. On the other hand, it measures the sensitivity of

*Author for correspondence (garciama@tandar.cnea.gov.ar).

One contribution of 17 to a Theme Issue 'Nonlinear dynamics in meso and nano scales: fundamental aspects and applications'.

a system to imperfect time inversion, i.e. evolve forward in time under H and then invert time and evolve backward with H_Σ (supposing that the time-inversion operation is not perfect).

Depending on the nature of the underlying dynamics, the LE can exhibit qualitatively different behaviour and it thus can be used to characterize quantum chaotic systems. Moreover, a number of time-reversal experiments have been performed [6–9], and therein lies the importance of the LE. In addition, the LE (which in quantum information is known as *fidelity*) can be efficiently measured in quantum information systems, i.e. its measurement scales only polynomially with the system size [10].

An important fact to remark is that quantum systems cannot be isolated easily. Most of the times, there is an environment acting upon the system. This interaction is most probably unknown and its effects may be uncontrollable. The Boltzmann echo (BE) was introduced [11] as a generalization of the LE to take into account the fact that quantum systems are not isolated. The idea is to consider the evolution of a system s with a Hamiltonian H_s that is coupled to an environment e whose evolution is given by H_e. We suppose the evolution of the environment e is unknown and are therefore uncontrollable, so we trace out the environment degrees of freedom. Given a separable initial state, such as $\rho_0 = \rho_0^{(\mathrm{s})} \otimes \rho_0^{(\mathrm{e})}$, where we take $\rho_0^{(\mathrm{s})} = |\psi_0\rangle\langle\psi_0|$, the BE is defined as the partial fidelity

$$M_\mathrm{B}(t) = \left\langle \langle\psi_0|\mathrm{Tr}_\mathrm{e}[\mathrm{e}^{-\mathrm{i}H_\mathrm{b}t/\hbar}\mathrm{e}^{-\mathrm{i}H_\mathrm{f}t/\hbar}\rho_0\mathrm{e}^{\mathrm{i}H_\mathrm{f}t/\hbar}\mathrm{e}^{\mathrm{i}H_\mathrm{b}t\hbar}]|\psi_0\rangle \right\rangle, \tag{1.2}$$

where H_b and H_f are given by

$$H_\mathrm{f} = H_\mathrm{s} \otimes \mathbb{I}_\mathrm{e} + \mathbb{I}_\mathrm{s} \otimes H_\mathrm{e} + U_\mathrm{f} \tag{1.3}$$

and

$$H_\mathrm{b} = -(H_\mathrm{s} + \Sigma_\mathrm{s}) \otimes \mathbb{I}_\mathrm{e} + \mathbb{I}_\mathrm{s} \otimes -(H_\mathrm{e} + \Sigma_\mathrm{e}) + U_\mathrm{b}, \tag{1.4}$$

which represent the forward and backward Hamiltonian, respectively. Equation (1.2) can be explained as follows. First take an initial state ρ_0 and evolve it forward up to time t with Hamiltonian H_f. Then, invert time evolution and evolve with Hamiltonian H_b. The imperfection in the inverting process is represented by: Σ_s for the system and Σ_e for the environment. The terms U_f and U_b represent forward and backward interactions between the system and environment (for simplicity throughout this work, we consider $U_\mathrm{f} = -U_\mathrm{b}$). Finally, the evolution of the system and the BE is obtained by performing a partial trace over the environment degrees of freedom and computing the overlap. Tracing out the environment makes the effective evolution of the system non-unitary producing decoherence [12]. An average over initial states of the environment $\rho_0^{(\mathrm{e})}$ is necessary (represented with big brackets in equation (1.2)) because we have no control over its degrees of freedom.

In the work of Petitjean & Jacquod [11], the BE was studied semiclassically for two interacting—classically chaotic—sub-systems. One of them was used as a system and the other as an environment. They found three different regimes for the BE as a function of time: parabolic or Gaussian for very short times, exponential for intermediate, followed by a saturation depending on the effective Hilbert space size. Here, we focus on the exponential regime and specifically on the

dependence of the decay rate on the perturbations and environment parameters. The authors show ([11], see also [5]) that in the Fermi golden rule (FGR) regime (small perturbations and weak coupling with the environment), the decay rate of the BE results from the sum of the decay rates of the LE owing to imperfect time inversion (by definition, the BE in the limit of no decoherence is just the LE), and the contribution owing to the interaction U_f and U_b with the environment, $\Gamma = \Gamma_{\Sigma_\mathrm{s}} + \Gamma_\mathrm{f} + \Gamma_\mathrm{b}$. Henceforth, we call this the *sum law*. Moreover, for chaotic systems, they find that in the limit of strong environment coupling or large perturbation, the decay rate is perturbation independent and is given by the classical Lyapunov exponent.

In the present contribution, we study the BE for quantum maps on the torus that are classically chaotic. Quantum maps are very simple models that have all the main features of chaotic systems and are ideal for numerical studies. Our goal is to understand the behaviour of the BE under the action of different environments. For this reason, we have computed the decay of the BE for a wide range of the parameters that control the perturbation of the system and the interaction with the environment. We find that a sum law for the decay rate of the BE exists. It can be expressed as the sum of the decay rates of the LE and the purity of the system, but it is fulfilled only partially, depending on the decoherence model. The decoherence models that we present can be written as a convolution with a kernel. It is for the cases where the kernels have polynomially decaying tails—models with somewhat large correlations in phase space—when the sum law is best achieved. In addition, the oscillations of the decay rate of the LE, found in e.g. Wang [13], Andersen [14] and Ares & Wisniacki [15], are damped completely in the limit of strong decoherence. However, the decoherence (and perturbation) independent decay-rate saturation at the classical Lyapunov exponent is not present for all decoherence models.

The paper is organized as follows. In §2*a*, we describe the quantum kicked maps on the torus, the systems used for our studies. Then in, §2*b*, we introduce our model of open maps using translations in phase space and the Kraus operator sum form. The main part of this contribution is §3, which is devoted to the numerical calculations and presentation of the results. Finally, in §4 we summarize our work and results.

2. The system

(*a*) *Quantum 'kicked' maps*

Classical maps generally arise from the discretization of a differential equation of the motion—e.g. a Poincaré surface of section. Nevertheless, one can build abstract maps that do not necessarily relate to a differential equation, but that can, however, provide insight into the properties of chaotic dynamics—e.g. the baker's map or the cat map. Like classical maps, quantum maps are usually simple operators with all typical properties of quantum chaotic systems such as level spacing statistics. In addition, there exist efficient quantum algorithms for some quantum maps (e.g. [16,17]). As the Hilbert space grows exponentially with the number of qubits, one could reach the semiclassical limit with a relatively small number of qubits. For this reason, they are ideal testbeds for current quantum computers in one of their possible uses: quantum simulators (see [18]).

The systems we consider are quantum maps on the 2-torus. Periodic boundary conditions imply that Hilbert space has the finite dimension N, and the effective Planck constant is $\hbar = 1/2\pi N$. This means that the semiclassical limit is reached as $N \to \infty$. Position and momentum bases are discrete sets $\{q_i = i/N\}_{i=0}^{N-1}$ and $\{p_i = i/N\}_{i=0}^{N-1}$ related by the discrete Fourier transform

$$\langle p|q\rangle = \frac{1}{\sqrt{N}} \mathrm{e}^{-(2\pi \mathrm{i} N)pq}. \tag{2.1}$$

For practical purposes, we will consider maps that can be expressed as two shears—linear or non-linear

$$\left.\begin{aligned} p' &= p - \frac{\mathrm{d}V(q)}{\mathrm{d}q} \pmod 1 \\ \text{and} \qquad q' &= q - \frac{\mathrm{d}T(p')}{\mathrm{d}p'} \pmod 1. \end{aligned}\right\} \tag{2.2}$$

These maps can be quantized, and the associated unitary map can be written as a product of two 'kicks'

$$U = \mathrm{e}^{\mathrm{i}2\pi N T(p)} \mathrm{e}^{-\mathrm{i}2\pi N V(q)}. \tag{2.3}$$

These types of map usually arise from Hamiltonians with periodic delta-kicks, like the kicked rotator [19] or the kicked Harper Hamiltonian [20]. One of the advantages of implementing these types of maps numerically is the possibility of using the fast Fourier transform.

(*b*) *Open quantum maps*

A system with an evolution given by a map U might interact with another system acting as an environment. If the dynamics of the environment cannot be accessed or controlled, then the usual procedure is to trace out the degrees of freedom of the environment. Tracing out the environment translates into a loss information about the evolution, hence the word *open*—we picture information flowing out of the system. It is this loss of information that is the cause of decoherence—and subsequent loss of *quantumness* [12]. The evolution can be described by a map of density matrices into density matrices. If the map is trace preserving and completely positive, then it can be put in the Kraus operator sum form [21]

$$\rho_t = \sum_i K_i(t) \rho_0 K_i(t)^\dagger. \tag{2.4}$$

If the environment is Markovian, i.e. memoryless, then the Kraus operators K_i are time independent, and equation (2.4) is further simplified as follows:

$$\rho_t = \sum_i K_i \rho_{t-1} K_i^\dagger, \tag{2.5}$$

where trace preservation is assured by $\sum_i K_i^\dagger K_i = I$ (I is the identity).[1] Here, we assume that the Markov approximation holds. Therefore, the action of the environment is coded into the Kraus operators K_i, in analogy with the Lindblad master equation [22] where the action of the environment is given by the Lindblad operators. Different Kraus operators will give different types of environments. Rather than modelling the environment through the Lindblad operators and solving the master equation, here we directly model the effect of the environment on the density matrix of the system by

$$\rho_t \stackrel{\text{def}}{=} \mathbf{D}_\epsilon(\rho_{t-1}) = \sum_{p,q=0}^{N-1} c_\epsilon(q,p)\, T_{qp} \rho_{t-1} T_{qp}^\dagger, \tag{2.6}$$

where T_{qp} are the translation operators on the torus, $c_\epsilon(q,p)$ is a function of q and p and ϵ quantifies the strength of the system–environment coupling. Even though position and momentum operators with canonical commutation rules are not defined on the torus, translations *can* be defined as cyclic shifts over the bases elements [23]. Since T_{qp} are unitary, trace preservation in equation (2.6) requires that $\sum_{q,p} c_\epsilon(q,p) = 1$. The action decoherence superoperator $\mathbf{D}_\epsilon$ introduced by equation (2.6) has a simple interpretation: it implements every possible translation in phase space with probability $c_\epsilon(q,p)$. This effect is clear in the Wigner function representation. Let $W(q,p)$ be the discrete Wigner function (e.g. [24]) of a density matrix ρ, then equation (2.6) can be rewritten as a convolution with $c_\epsilon(q,p)$

$$W_t(Q,P) = \sum_{q,p} c_\epsilon(q,p)\, W_{t-1}(Q-q, p-P). \tag{2.7}$$

This is an incoherent sum of slightly displaced Wigner functions. Any fast oscillating term present in the state represented by $W(q,p)$ will be eventually washed out, depending on the form of $c_\epsilon(q,p)$.

For simplicity, we suppose that the complete evolution of the quantum map and the decoherent part take place in two steps: first the unitary map U, then the decoherence term of equation (2.6)

$$\rho_t = \mathbf{D}_\epsilon(U \rho_{t-1} U^\dagger). \tag{2.8}$$

This is an approximation that works exactly in some cases, e.g. a billiard that has elastic collisions on the walls and diffusion in the free evolution between collisions. This kind of two-step model has been used to study quantum to classical correspondence and the emergence of classical properties from quantum dynamics [25,26].

The effect of decoherence can be characterized by using the purity

$$P(t) = \mathrm{tr}(\rho_t^2), \tag{2.9}$$

where ρ_t is the reduced density matrix of the system. The purity measures the relative weight of the non-diagonal matrix elements. It is a basis independent measure that can be used to quantify the amount of entanglement between two

[1]Throughout this contribution, the 'time' t is a discrete time variable that implies the number of times a map (or a superoperator) has been applied.

parties. If $P(t)=1$, it means that the global system can be factorized into two separate systems and there is no entanglement. On the contrary, if the purity of the reduced density matrix is minimum (completely mixed state), then the entanglement is maximal. In the case of an N-dimensional system, $P(t)=1/N$ for a completely mixed state (maximally entangled with the environment). As a function of time, after an initial short transient, the purity decays exponentially (see [5,12] and references therein). For long times, it saturates to a minimum value given by $\hbar/(2\pi)$.

3. Numerical results

For our numerical calculations, we use the cat map perturbed in position and momentum with a smooth nonlinear shear

$$\left.\begin{aligned} p' &= p + a\,q - 2\pi k \sin(2\pi q) \pmod 1 \\ \text{and}\qquad q' &= q + b\,p' - 2\pi k \sin(2\pi p') \pmod 1, \end{aligned}\right\} \tag{3.1}$$

where a and b are integers. This map is uniformly hyperbolic and fully chaotic. For $k \ll 1$ the largest Lyapunov exponent given by $\lambda \approx \ln((2+ab+\sqrt{ab(4+ab)})/2)/2$. According to equation (2.3), the quantum version of equation (3.1) is

$$U_k = \mathrm{e}^{2\pi \mathrm{i}(-P^2/(2N) - k\cos(2\pi P/N))}\, \mathrm{e}^{2\pi \mathrm{i}(Q^2/(2N) + k\cos(2\pi Q/N))}, \tag{3.2}$$

where $P, Q = 0, \ldots, N-1$. All the arithmetic peculiarities of the cat map, which account for the non-generic spectral statistics are destroyed for $k \neq 0$ [27,28]. We can rewrite equation (1.2) for the BE for our open map as the overlap between two states evolving forward in time—with slightly different maps plus decoherence—as

$$M_{\mathrm{B}}(t) = \mathrm{Tr}[\bar{\rho}_t \rho_t], \tag{3.3}$$

where

$$\rho_t = \mathbf{D}_\epsilon(U_k \rho_{t-1} U_k^\dagger) \tag{3.4}$$

and

$$\bar{\rho}_t = \mathbf{D}_\epsilon(U_{k'} \rho_{t-1} U_{k'}^\dagger), \tag{3.5}$$

where k and k' are the perturbation strength of the cat map. We measure the perturbation of one map with respect to the other by the parameter

$$\Sigma \equiv |k' - k|. \tag{3.6}$$

For a chaotic system, after an initial transient, the BE decays exponentially [5]. Here, we focus on the decay rate Γ as a function of Σ and ϵ for the exponential decay regime. In the limit $\epsilon \to 0$, we have $\Gamma = \Gamma_\Sigma$, where Γ_Σ is the decay rate of the LE. In the limit $\Sigma \to 0$, the BE as defined in equation (3.3) is equal to the purity, so the decay rate is given by the decay rate of the purity Γ_ϵ.

We explore the behaviour of Γ for three decoherence models and a wide range of values of ϵ and Σ. We analyse the parameter domain of validity of the sum law (now $\Gamma = \Gamma_\Sigma + \Gamma_\epsilon$) for these models. The different models of decoherence we consider are implemented simply by changing the coefficients $c_\epsilon(q,p)$ in

equation (2.6). As for the LE, to extract the decay rate Γ, an average over an ensemble of initial states needs to be performed. For the averages, we used $n_s = 10$ randomly chosen coherent states.

(a) Gaussian diffusion

The first model we have considered was introduced in the work of García-Mata *et al.* [29] to model diffusion in a quantum map. We take a periodic sum of Gaussians—to fit the boundary conditions of the 2-torus

$$c_\epsilon(q,p) = \frac{1}{A}\sum_{j,k=-x}^{x} \exp\left[-\frac{(q-jN)^2+(p-kN)^2}{2\,(\epsilon N/2\pi)^2}\right], \tag{3.7}$$

where x is large enough (typically of order 10–15) so that the tails of the furthermost Gaussians can be neglected and A is the normalization factor $(q,p=0,\ldots,N-1)$. We call this model the Gaussian diffusion model (GDM). The GDM can be interpreted as a smoothing or coarse graining of the unitary evolution: with Gaussian weight, the state is displaced all over a region of size of order ϵ. As a consequence, the interference terms get washed out, while the remaining classical part is diffused. As stated before, in the continuous limit, equation (2.7) is a convolution of the Wigner function with a kernel $c_\epsilon(q,p)$. For the GDM, it can be related to the solution of the heat equation with a diffusion constant given by $(\epsilon/2\pi)^2$ [30–33].

In figure 1*a*, we show the decay rate Γ of the BE as a function of perturbation parameter Σ for the perturbed cat map $a=b=2$, $N=800$ and $k=0.01$ in the presence of the GDM for distinct values of ϵ. The Lyapunov exponent $\lambda = \ln[3+2\sqrt{2}]$ is marked by a dashed line. For $\epsilon = 0$ (cross symbols), we recover the decay rate of the LE: for small Σ, we get the characteristic quadratic behaviour for small perturbations—FGR regime; for larger values of Σ, we get a non-universal—perturbation dependent—oscillatory behaviour that has also been observed in the work of Wang *et al.* [13] and Ares & Wisniacki [15,34]. As ϵ increases, the initial Γ value tends to increase (giving the characteristic exponential decay of the purity rate owing to decoherence), while the amplitude of the oscillations seems to decrease approaching the value of the classical Lyapunov exponent.

In figure 1*b*, the decay rate of the purity Γ_ϵ, which corresponds to the BE for $\Sigma = 0$, is shown. The symbols correspond to the curves—for different ϵ values—in figure 1*a*. For the GDM, we observe saturation of Γ_ϵ at λ, as is expected. In the inset, we assess the sum law $\Gamma \sim \Gamma_\epsilon + \Gamma_\Sigma$ for the BE, and we plot $\Gamma - \Gamma_\epsilon$ as a function of $\Sigma/\hbar$: the expected behaviour—all curves collapsing into the one corresponding to Γ_Σ—is only observed for values of $\epsilon \lesssim 0.0035$ corresponding to $\Gamma_\epsilon \lesssim 0.5$. For $\epsilon = 0.0035$ (diamonds), we see that the sum law breaks up around $\Sigma/\hbar \approx 0.75$. For $\epsilon \gtrsim 0.0035$, the sum law is no longer valid.

(b) Generalized depolarizing channel

The next environment model that we have considered is the generalized depolarizing channel (DC). Although—as we shall see—in phase space it is somehow an extremely non-local noise, its importance lies in that it is one of the

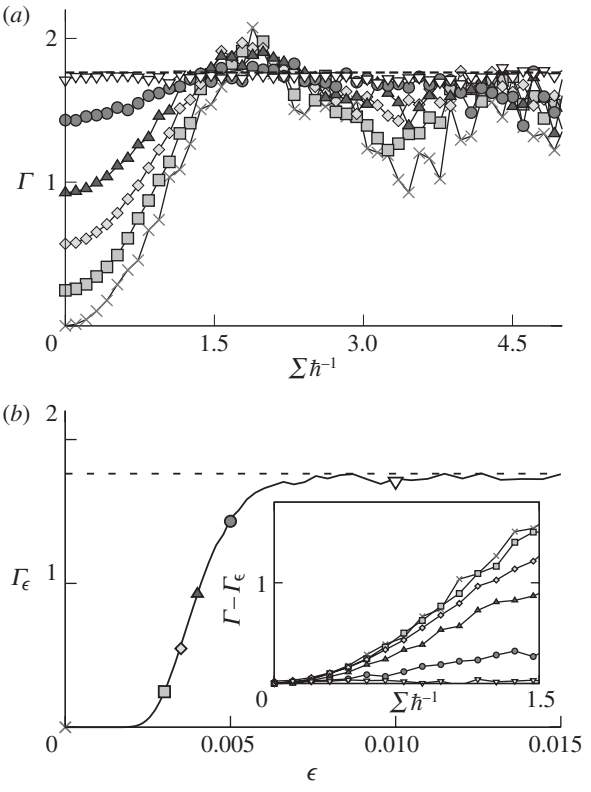

Figure 1. (*a*) Decay rate Γ of the BE as a function of the rescaled strength of the perturbation $\Sigma/\hbar$ for a GDM environment. The map is the quantum version of the perturbed cat (equation (3.1)), with $a = b = 2$. Averages were done over $n_s = 10$ initial states. Other parameters are: $k = 0.001$, $N = 800$. Cross symbols, $\epsilon = 0$ (LE); squares, $\epsilon = 0.003$; diamonds, $\epsilon = 0.0035$; triangles, $\epsilon = 0.004$; circles, $\epsilon = 0.005$; inverted triangles, $\epsilon = 0.01$. The horizontal dashed lines (in (*a*) and (*b*)) correspond to the Lyapunov exponents of the corresponding map $\lambda = \ln[3 + 2\sqrt{2}] \approx 1.76275$. (*b*) The decay rate Γ_ϵ of the purity as a function of the perturbation parameter ϵ. The points correspond to the initial values of the curves in (*a*). (inset) Decay rate $\Gamma - \Gamma_\epsilon$ as a function of the rescaled strength of the perturbation $\Sigma/\hbar$.

simplest and the best-known noise channels in quantum-information formalism [35]. The action of the DC for one qubit ($N = 2$) is simple: with probability $(1 - \epsilon)$, it does nothing, and with probability ϵ, it 'depolarizes' it, meaning that it leaves it in a completely mixed state. This is done by applying every possible Pauli matrix on the state. For an N-dimensional system and a torus phase space, it can be generalized as follows [36]:

$$\mathbf{D}_\epsilon^{\mathrm{DC}} = (1 - \epsilon)\rho + \frac{\epsilon}{N^2} \sum_{q,p \neq 0} T_{qp} \rho T_{qp}^\dagger, \tag{3.8}$$

that is, with probability $(1 - \epsilon)$, it leaves the state unchanged, while with probability ϵ, it applies every possible translation in phase space, with equal weight ϵ/N^2. So, contrary to the GDM where the incoherent sum over displaced

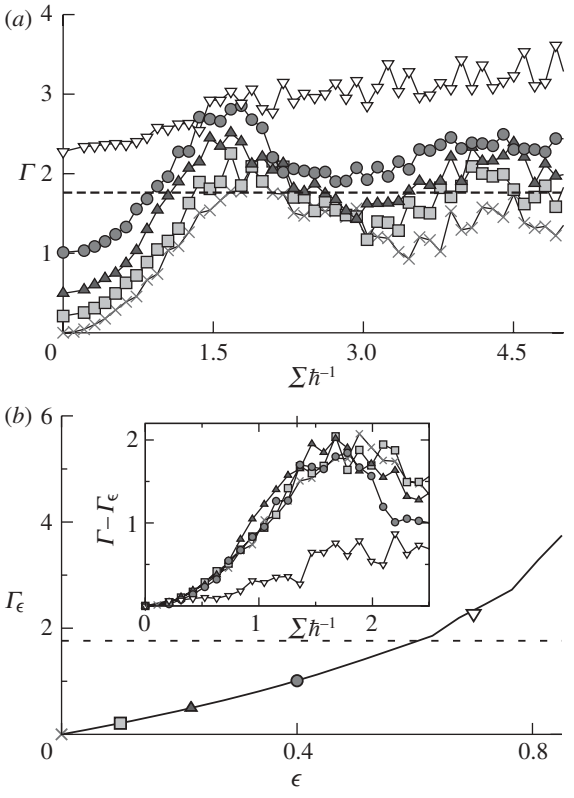

Figure 2. (*a*) Decay rate Γ of the BE as a function of the rescaled strength of the perturbation $\Sigma/\hbar$ for a DC environment. The map is the quantum version of the perturbed cat (equation (3.1)), with $a = b = 2$. Averages were done over $n_s = 10$ initial states. Other parameters are: $k = 0.001$, $N = 800$. Cross symbols, $\epsilon = 0$ (LE); squares, $\epsilon = 0.1$; triangles, $\epsilon = 0.22$; circles, $\epsilon = 0.40$; inverted triangles, $\epsilon = 0.7$. The horizontal dashed lines (in (*a*) and (*b*)) correspond to the Lyapunov exponents of the corresponding maps $\lambda = \ln[3 + 2\sqrt{2}] \approx 1.76275$. (*b*) The decay rate Γ_ϵ of the purity as a function of the perturbation parameter ϵ. The points correspond to the initial values of the curves in (*a*). (inset) Decay rate $\Gamma - \Gamma_\epsilon$ as a function of the rescaled strength of the perturbation $\Sigma/\hbar$.

states took place between states lying effectively close, owing to the Gaussian weight, for the DC, the incoherent sum is over all states, close or apart. It is in this sense that we say this model is highly non-local.

In figure 2*a*, we show the BE decay rate Γ as function of perturbation parameter Σ for the perturbed cat map $a = b = 2$, $N = 800$ and $k = 0.01$ in the presence of the DC noise model for distinct values of ϵ. Again, the cross symbols represent the Γ_Σ of the LE. For smaller ϵ, the curves look like essentially the same curve shifted upwards. There is no evident saturation at the Lyapunov exponent. For a larger ϵ, the BE oscillations tend to disappear, and the growth is somehow linear with no apparent saturation. In figure 2*b*, we show the decay rate of the purity Γ_ϵ as a function of ϵ and the symbols mark the initial values of the curves on the top. Initially, Γ_ϵ grows linearly. As is expected [34], there is no parameter-independent regime for the DC observed, neither for Γ nor for Γ_ϵ. In the inset of

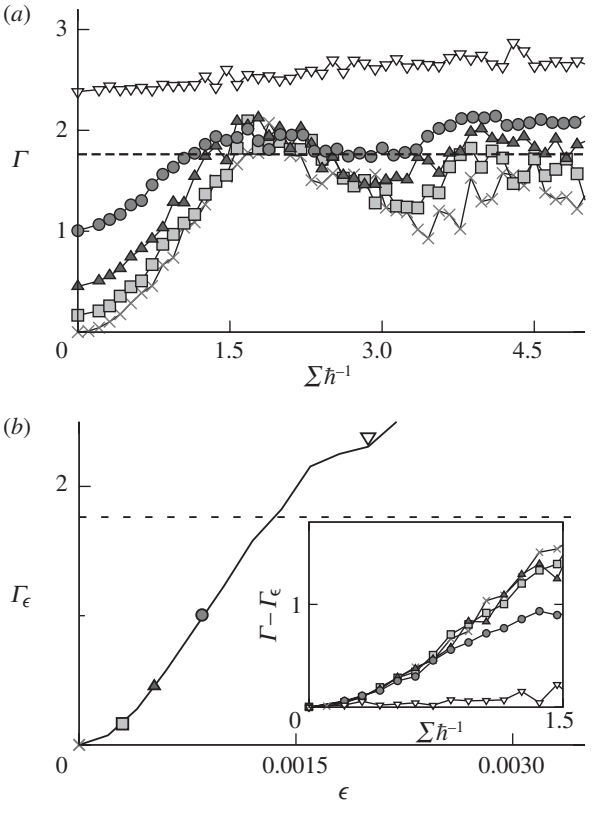

Figure 3. (*a*) Decay rate Γ of the BE as a function of the rescaled strength of the perturbation $\Sigma/\hbar$ for an LDM environment. The map is the quantum version of the perturbed cat (equation (3.1)), with $a = b = 2$. Averages were done over $n_s = 10$ initial states. Other parameters are: $k = 0.001$, $N = 800$. Cross symbols, $\epsilon = 0$ (LE); squares, $\epsilon = 0.001$; triangles, $\epsilon = 0.002$; circles, $\epsilon = 0.005$; inverted triangles, $\epsilon = 0.01$. The horizontal dashed lines (in (*a*) and (*b*)) correspond to the Lyapunov exponents of the corresponding map $\lambda = \ln[3 + 2\sqrt{2}] \approx 1.76275$. (*b*) The decay rate Γ_ϵ of the purity as a function of the perturbation parameter ϵ. The points correspond to the initial values of the curves in (*a*). (inset) Decay rate $\Gamma - \Gamma_\epsilon$ as a function of the rescaled strength of the perturbation $\Sigma/\hbar$.

figure 2, we show the decay rate of $\Gamma - \Gamma_\epsilon$. We can see the lines collapse to the curve corresponding to Γ_Σ (cross symbols) for the LE for a sizeable interval of $\Sigma/\hbar$ and up to values of $\Gamma_\epsilon \approx 1$. From the work by Casabone *et al.* [34], we know that the decay rate of purity as a function of ϵ is $\Gamma_\epsilon = 2\epsilon$, for small ϵ. It is simple to show that in the interval of ϵ where this holds, the sum law $\Gamma_\Sigma \approx \Gamma - \Gamma_\epsilon$ also holds. Here, this is true up to values $\epsilon \lesssim 0.4$ (see also fig. 2 in [34]) corresponding to $\Gamma_\epsilon \lesssim 1$.

(*c*) *Lorentzian decoherence*

Finally, we consider a model that is more local than the DC but which, unlike the GDM, has polynomially decaying tails for $c_\epsilon(q, p)$. The motivation for using this model arose in the work by Casabone *et al.* [34] when comparing

the universalities of the purity and the LE. We take $c_\epsilon(q,p)$ to be a sum of Lorentzians

$$c_\epsilon(q,p) = \frac{1}{\pi A} \sum_{j,k=-x}^{x} \frac{\epsilon N/2\pi}{\left((\epsilon N/2\pi)^2 + (q - Nj)^2 + (p - Nk)^2\right)}, \tag{3.9}$$

with A the proper normalization for $\sum_{q,p} c_\epsilon(q,p) = 1$ and $q,p = 0,\ldots,N-1$. The sum is done to account for the periodicity of the torus (theoretically, $x \to \infty$; practically, x is an integer much larger than 1). We call this model the Lorentz decoherence model (LDM). Equation (2.6) with $c_\epsilon(q,p)$ given by equation (3.9) defines a random process with Lorentzian weight that can be related to superdiffusion by Lévy flights. The effect of heavy tails in decoherence is also explored in e.g. the work of Schomerus & Lutz [37].

In figure 3*a*, we show the decay rate Γ of the BE as a function of perturbation parameter Σ for the perturbed cat map $a = b = 2$, $N = 800$ and $k = 0.01$, in the presence of the LDM for different ϵ values. Again, we see that for small ϵ, the curves look like a shift of one another—although less so than for the DC model—and then for large values of ϵ, the oscillations are destroyed and the growth of Γ is linear, as for the DC. Figure 3*b* shows the decay rate Γ_ϵ of the purity with the initial points of the curves on the top superimposed. The initial growth of Γ_ϵ is quadratic with ϵ, as was shown in Casabone *et al.* [34]. It can also be clearly observed that in neither figure there is a parameter-independent—Lyapunov—regime. In the inset of figure 3, we show the decay rate $\Gamma - \Gamma_\epsilon$. The sum law $\Gamma_\Sigma \sim \Gamma - \Gamma_\epsilon$ holds for an interval of $\Sigma/\hbar$ up to $\Sigma/\hbar \approx 1.5$ (similar to the DC case), but it seems to break up a little bit earlier in the values of Γ_ϵ. Note that in the inset of figure 3*b*, the line corresponding to the circles ($\Gamma_\epsilon \approx 1$) separates from the others at $\Sigma/\hbar \approx 0.75$.

4. Conclusions

Summarizing, we have studied the BE for quantum chaotic maps with three different types of decoherence. The BE complements the original idea of the LE in that it considers the presence of an environment, yielding it appropriate for understanding the realistic experiments. We have done extensive numerical calculations for a wide range of values of the perturbation of the map and the strength of the decoherence superoperator, and we have focused on the decay rate of the BE in the regime where it decays exponentially. Other than providing a 'visual landscape' of the decay rate Γ of the BE, our calculations enable a qualitative and quantitative analysis of the universal regimes found in the literature. We found that the more realistic diffusion model (GDM) correctly retrieves the Lyapunov behaviour for large enough values of ϵ. However, for the same case, the sum law $\Gamma \approx \Gamma_\Sigma + \Gamma_\epsilon$ breaks up for relatively small values of ϵ. We infer that this problem is related to the fact that the Hilbert space associated to the torus is N-dimensional (similar non-universal behaviour is found for the purity in the work of Casabone *et al.* [34]). On the contrary, the two other cases considered satisfy the sum law rather well. These two models have in common the slow decaying tails of the kernel $c_\epsilon(q,p)$, which means that the decoherence model acts non-locally in phase space. Furthermore, these two models fail to exhibit the parameter-independent Lyapunov regime.

We have used quantum maps as generic chaotic systems and three very different decoherence models. We can thus conclude that non-generic behaviour is to be expected in echo experiments with arbitrary types of environment.

The authors acknowledge financial support from CONICET (PIP-6137), UBACyT (X237) and ANPCyT. D.A.W. and I.G.-M. are researchers of CONICET.

References

1 Peres, A. 1984 Stability of quantum motion in chaotic and regular systems. *Phys. Rev. A* **30**, 1610–1615. (doi:10.1103/PhysRevA.30.1610)

2 Jalabert, R. A. & Pastawski, H. M. 2001 Environment-independent decoherence rate in classically chaotic systems. *Phys. Rev. Lett.* **86**, 2490–2493. (doi:10.1103/PhysRevLett.86.2490)

3 Jacquod, P., Silvestrov, P. G. & Beenakker, C. W. J. 2001 Golden rule decay versus Lyapunov decay of the quantum Loschmidt echo. *Phys. Rev. E* **64**, 055203(R). (doi:10.1103/PhysRevE.64.055203)

4 Gorin, T., Prosen, T., Seligman, T. & Žnidarič, M. 2006 Dynamics of Loschmidt echoes and fidelity decay. *Phys. Rep.* **435**, 33–156. (doi:10.1016/j.physrep.2006.09.003)

5 Petitjean, C. & Jacquod, P. 2009 Decoherence, entanglement and irreversibility in quantum dynamical systems with few degrees of freedom. *Adv. Phys.* **58**, 67–196. (doi:10.1080/00018730902831009)

6 Hahn, E. L. 1950 Spin echoes. *Phys. Rev.* **80**, 580–594. (doi:10.1103/PhysRev.80.580)

7 Rhim, W.-K., Pines, A. & Waugh, J. S. 1970 Violation of the spin-temperature hypothesis. *Phys. Rev. Lett.* **25**, 218–220. (doi:10.1103/PhysRevLett.25.218)

8 Zhang, S., Meier, B. H. & Ernst, R. R. 1992 Polarization echoes in NMR. *Phys. Rev. Lett.* **69**, 2149–2151. (doi:10.1103/PhysRevLett.69.2149)

9 Pastawski, H. M., Levstein, P. R., Usaj, G., Raya, J. & Hirschinger, J. 2000 A nuclear magnetic resonance answer to the Boltzmann Loschmidt controversy? *Physica A* **283**, 166–170. (doi:10.1016/S0378-4371(00)00146-1)

10 Emerson, J., Weinstein, Y. S., Lloyd, S. & Cory, D. G. 2002 Fidelity decay as an efficient indicator of quantum chaos. *Phys. Rev. Lett.* **89**, 284102. (doi:10.1103/PhysRevLett.89.284102)

11 Petitjean, C. & Jacquod, P. 2006 Quantum reversibility and echoes in interacting systems. *Phys. Rev. Lett.* **97**, 124103. (doi:10.1103/PhysRevLett.97.124103)

12 Zurek, W. H. 2003 Decoherence, einselection, and the quantum origins of the classical. *Rev. Mod. Phys.* **75**, 715–775. (doi:10.1103/RevModPhys.75.715)

13 Wang, W.-G., Casati, G. & Li, B. 2004 Stability of quantum motion: beyond Fermi-golden-rule and Lyapunov decay. *Phys. Rev. E* **69**, 025201(R). (doi:10.1103/PhysRevE.69.025201)

14 Andersen, M. F., Kaplan, A., Grunzweig, T. & Davidson, N. 2006 Decay of quantum correlations in atom optics billiards with chaotic and mixed dynamics. *Phys. Rev. Lett.* **97**, 104102. (doi:10.1103/PhysRevLett.97.104102)

15 Ares, N. & Wisniacki, D. A. 2009 Loschmidt echo and the local density of states. *Phys. Rev. E* **80**, 046216. (doi:10.1103/PhysRevE.80.046216)

16 Georgeot, B. & Shepelyansky, D. L. 2001 Stable quantum computation of unstable classical chaos. *Phys. Rev. Lett.* **86**, 5393–5396. (doi:10.1103/PhysRevLett.86.5393)

17 Lévy, B., Georgeot, B. & Shepelyansky, D. L. 2003 Quantum computing of quantum chaos in the kicked rotator model. *Phys. Rev. E* **67**, 046220. (doi:10.1103/PhysRevE.67.046220)

18 Schack, R. 2006 Simulation on a quantum computer. *Informatik–Forschung und Entwicklung* **21**, 21–27. (doi:10.1007/s00450-006-0010-0)

19 Chirikov, B., Izrailev, F. & Shepelyansky, D. L. 1988 Quantum chaos: localization vs. ergodicity. *Physica D* **33**, 77–88. (doi:10.1016/S0167-2789(98)90011-2)

20 Leboeuf, P., Kurchan, J., Feingold, M. & Arovas, D. 1990 Phase-space localization: topological aspects of quantum chaos. *Phys. Rev. Lett.* **65**, 3076–3079. (doi:10.1103/PhysRevLett.65.3076)

21 Kraus, K. 1983 *States, Effects and Operations*. Berlin, Germany: Springer.

22 Lindblad, G. 1976 On the generators of quantum dynamical semigroups. *Commun. Math. Phys.* **48**, 119–130. (doi:10.1007/BF01608499)
23 Schwinger, J. 1960 Unitary operator bases. *Proc. Natl Acad. Sci. USA* **46**, 570–579. (doi:10.1073/pnas.46.4.570)
24 Bianucci, P., Miquel, C., Paz, J. P. & Marcos Saraceno, M. 2002 *Phys. Lett. A* **297**, 353–358. (doi:10.1016/S0375-9601(02)00391-2)
25 García-Mata, I. & Saraceno, M. 2004 Spectral properties and classical decays in quantum open systems. *Phys. Rev. E* **69**, 056211. (doi:10.1103/PhysRevE.69.056211)
26 Nonnenmacher, S. 2003 Spectral properties of noisy classical and quantum propagators. *Nonlinearity* **16**, 1685–1713. (doi:10.1088/0951-7715/16/5/309)
27 Basilio de Matos, M. & Ozorio de Almeida, A. M. 1995 Quantization of Anosov maps *Ann. Phys.* **237**, 46–65. (doi:10.1006/aphy.1995.1003)
28 Keating, J. P. & Mezzadri, F. 2000 Pseudo-symmetries of Anosov maps and spectral statistics. *Nonlinearity* **13**, 747–775. (doi:10.1088/0951-7715/13/3/313)
29 García-Mata, I., Saraceno, M. & Spina, M. E. 2003 Classical decays in decoherent quantum maps. *Phys. Rev. Lett.* **91**, 064101. (doi:10.1103/PhysRevLett.91.064101)
30 Zurek, W. H. & Paz, J. P. 1994 Decoherence, chaos and the second law. *Phys. Rev. Lett.* **72**, 2508–2511. (doi:10.1103/PhysRevLett.72.2508)
31 Strunz, W. T. & Percival, I. C. 1998 Classical mechanics from quantum state diffusion—a phase-space approach. *J. Phys. A* **31**, 1801. (doi:10.1088/0305-4470/31/7/014)
32 Carvalho, A. R. R., de Matos Filho, R. L. & Davidovich, L. 2004 Environmental effects in the quantum-classical. *Phys. Rev. E* **70**, 026211. (doi:10.1103/PhysRevE.70.026211)
33 Wisniacki, D. A. & Toscano, F. 2009 Scaling laws in the quantum-to-classical transition in chaotic systems. *Phys. Rev. E* **79**, 025203(R). (doi:10.1103/PhysRevE.79.025203)
34 Casabone, B., García-Mata, I. & Wisniacki, D. A. 2010 Discrepancies between decoherence and the Loschmidt echo. *Europhys. Lett.* **89**, 50009. (doi:10.1209/0295-5075/89/50009)
35 Nielsen, A. & Chuang, I. L. 2000 *Quantum computation and quantum information*. Cambridge, UK: Cambridge University Press.
36 Aolita, M. L., Garcia-Mata, I. & Saraceno, M. 2004 Noise models for superoperators in the chord representation. *Phys Rev. A* **70**, 062301. (doi:10.1103/PhysRevA.70.062301)
37 Schomerus, H. & Lutz, E. 2007 Nonexponential decoherence and momentum subdiffusion in a quantum Lévy kicked rotator. *Phys. Rev. Lett.* **98**, 260401. (doi:10.1103/PhysRevLett.98.260401)